Dependence of photon-atom scattering on energy resolution and target angular momentum

J. P. J. Carney and R. H. Pratt
Department of Physics and Astronomy, University of Pittsburgh, Pittsburgh, Pennsylvania 15260

N. L. Manakov and A. V. Meremianin
Department of Physics, Voronezh State University, Voronezh 394693, Russia
(Received 7 September 1999; published 6 March 2000)

We consider a more correct treatment of photon scattering from randomly oriented atoms, going beyond the level of description used in currently available results. We focus on cross sections which include an elastic scattering component. The most sophisticated results available to describe high-energy elastic scattering are relativistic coherent elastic *S*-matrix calculations within independent-particle approximation, which, however, perform an averaging over magnetic substates at the level of the amplitude (averaged-amplitude approach), exact only for fully filled subshells. The present *S*-matrix calculations also do not consider incoherent elastic scattering (in which an electron makes a transition to a different magnetic substate in the same subshell), which can occur when there are partially filled subshells. A more proper treatment of these situations involves an averaging over the cross sections for all possible orientations of the target. Here we consider the total elastic scattering (both coherent and incoherent), and we also include the unresolved contributions of inelastic (Raman and Compton) scattering. In particular we consider inelastic Raman scattering between relativistic subshells that are nearly energy degenerate, which may not be resolved, given finite experimental resolution, and which may be degenerate in nonrelativistic theory (e.g., Coulombic $2p_{1/2}$ and $2p_{3/2}$ subshells). Thus, for example, the nonrelativistic result for elastic scattering (coherent and incoherent) from excited hydrogen in the $2p$ state corresponds to the result obtained by summing relativistic elastic scattering (coherent and incoherent) together with the relativistic inelastic scattering for transitions between the $2p_{1/2}$ and $2p_{3/2}$ subshells. The averaged-amplitude approach does poorly in this case. However, results for scattering from ground-state boron indicate that the averaged-amplitude approach generally works well for many-electron ground-state atoms, due to the large coherent contribution from electrons in fully filled subshells.

PACS number(s): 32.80.Cy

I. INTRODUCTION

How to obtain accurate predictions for the elastic scattering of photons by atomic targets has long been and remains a subject of interest. See Refs. [1,2] for discussions of the various theoretical approaches and the comparison of theoretical predictions with experiment. In this paper we wish to go beyond the usual level of description, considering effects associated with partially filled subshells, and considering the consequences of finite energy resolution. Our particular interest here is in cross sections involving an elastically scattering component. The target is assumed to be randomly oriented, and final target orientations are not observed. We will discuss effects of approximations in averaging which have been used in describing the elastic (coherent and incoherent) scattering cross section. We will also discuss the inclusion of inelastic scattering cross sections, needed to correspond to an experimental observation of finite energy resolution, or to correspond to calculations in a simpler theory (e.g., nonrelativistic theory).

The most sophisticated calculations describing high-energy elastic scattering are based on the evaluation of the second-order *S*-matrix element in the atomic potential as described in Refs. [2,3], following the earlier work of Brown *et al.* [4] and Johnson and Feiock [5]. (The *S*-matrix approach has also been applied to the case of inelastic Compton scattering [6,7].) These are relativistic calculations in independent-particle approximation (IPA), retaining all significant multipoles in the electron-photon interaction, with electron orbitals being obtained in a local relativistic self-consistent Dirac-Slater type central potential. The regimes of validity of simpler approximations have often been determined by comparison with *S*-matrix calculations [1,8], and the *S*-matrix calculations have generally been regarded as benchmark calculations for elastic photon scattering from atoms in the x-ray and γ-ray regime. It therefore is of interest to understand how accurate these *S*-matrix results are. There have been investigations of photon polarization effects [9], the multipole dependence of scattering [10], and angular distributions [11], all depending in part on the *S*-matrix calculations.

There are corresponding analytic nonrelativistic *S*-matrix results: The problem of elastic scattering from hydrogenlike atoms has been investigated in detail using the nonrelativistic dipole approximation for the $n=1$ [12], $n=2$ [13–15], and $n=3$ [16] shells. In Ref. [17] analytic results are presented for Raman scattering between the $n=1$ and the $n=2,3$ shells, as well as for elastic scattering. Retardation effects [18,19] and relativistic effects [20,21] in scattering from hydrogenic *K*-shell electrons were also considered. In Ref. [22] numerical results are given for the cross section of elastic coherent Rayleigh scattering from the ground states of relativistic hydrogenlike ions with $Z=1$, 30, 50, and 80, and for relative contributions of retardation and relativistic effects. The inelastic (Raman) cross sections for transitions between $1s_{1/2}$ and excited $2s_{1/2}$, $2p_{1/2}$, and $2p_{3/2}$ states were also calculated.

We note the extensive theoretical tabulations of elastic scattering which have become available. Many tabulations are based on the form-factor approximation for describing elastic scattering, which is attractive because of its simplicity. There are extensive tabulations of form factors (FF's) using nonrelativistic [23] and relativistic [24] nonlocal wave functions, and also of modified form factors (MFF's) [25], which take account of additional electron binding effects. More recently *S*-matrix results for all elements, angles, and energies ranging from eV to MeV, as well as results based on the form-factor approximation and on form factors combined with anomalous scattering factors, have been made available online [26]. A tabulation has also been published, based on interpolation on previously published *S*-matrix results, for all elements in the range $13 \leqslant Z \leqslant 104$, all scattering angles, and photon energies in the range 50–1500 keV [27].

The *S*-matrix formalism presented in Refs. [2,3] is restricted to the case of elastic coherent Rayleigh scattering (exactly the same initial and final atomic state), and an averaging over all magnetic substate contributions at the level of the scattering amplitude (which we call the *averaged-amplitude* approach), weighted by the number of electrons in the subshell, is performed for each subshell. This procedure is exact only for fully filled subshells, where all the magnetic substates are occupied; it is approximate when the target has partially filled subshells, in which case there is both coherent and incoherent elastic scattering. Given our assumptions, we cannot distinguish between coherent and incoherent elastic scattering, since this would require making observations of the target. (We note that the same type of amplitude averaging is employed in the form factor tabulations [23–25].)

A more correct procedure is to calculate all cross sections for atoms with specified numbers of electrons in subshells, averaging over all possible initial orientations of the target, and summing over final orientations. This corresponds to averaging and summing the cross sections over all possible magnetic substate occupations. For each definite magnetic substate occupation, the coherent elastic amplitude is obtained by summing over the elastic scattering from each of the electrons. The incoherent amplitudes for transitions to unoccupied substates should be summed at the level of the cross section. The final result is obtained by averaging the cross sections for all possible initial magnetic substate occupations with the specified number of electrons in the subshell. This procedure takes account of incoherent elastic scattering, in which the initial and final states of the atom are different, though energy degenerate (i.e., corresponding to transitions within the same subshell). Incoherent elastic scattering is neglected in the averaged-amplitude approach. Note that for fully filled subshells this more correct procedure does lead to the averaged-amplitude result, as there is only one possible magnetic substate occupation (all substates occupied); the coherent summation is therefore over all magnetic substates, and there is no incoherent elastic scattering.

Our concern here is twofold: (1) How is the accuracy of the present independent-particle-approximation (IPA) *S*-matrix results for elastic scattering affected by the averaged-amplitude approximation, performing averaging at the level of the amplitude for partially filled subshells, and neglecting incoherent elastic scattering (present for partially filled shells)? (2) When should one include inelastic Raman scattering between different subshells that are nearly energy degenerate (e.g., $2p_{1/2}$ and $2p_{3/2}$ subshells for low Z), as is necessary to correspond to the nonrelativistic result for scattering, or to include inelastic Raman scattering into other shells and even Compton scattering, depending on the energy resolution involved?

Our discussion here will be more appropriate at higher energies, and/or higher Z, where independent-particle approximation can be justified. There have been recent investigations of the adequacy of IPA assumptions in the *S*-matrix results, examining consequences of nonlocal exchange and electron correlation, which become important at lower energies, and in lighter elements. Experimental results highlighted a discrepancy between these *S*-matrix predictions and experiment for scattering by neon for photon energies in the range 11–22 keV [28] (the *K*-shell threshold for neon is $\approx$870 eV). It was shown that corrections obtained from simple form-factor-based calculations could account for these differences in light elements in the above-threshold region [28]: the effect of correlations on the elastic scattering cross section was small, while nonlocal effects could change the elastic scattering cross section by as much as 10%, depending on the momentum transfer involved. (We shall return to these results [28] in Sec. II, as they also provide an example of how experimental energy resolution determines which inelastic cross sections must be included with the elastic scattering cross section.) In general the *S*-matrix results are also not expected to be accurate too close to resonances, where many-electron effects can be large and where finite level widths become important (the *S*-matrix calculation neglects level widths, leading to singularities which are removed when the finite widths are considered).

We find that the averaged-amplitude Rayleigh *S*-matrix approach can be expected to provide a good description of elastic scattering from randomly oriented middle- to high-Z ground-state atoms, for photon energies in the x-ray and γ-ray regime (assuming one is including the coherent nuclear and Delbrück amplitudes when appropriate). This is because the elastic coherent amplitude is a coherent sum of the contributions from all electrons, most of which are in fully filled subshells, and this accounts for most of the scattering cross section. The form-factor-type contribution from the valence electrons is dropping much faster with increasing angle than the innershell amplitudes (given that we have photon energies above the innershell thresholds and well above the valence-shell thresholds), leading to the (fully filled) innershell amplitudes being dominant at finite angles. At forward angle the valence electrons contribute significantly but the form factor at forward angle is the same whether one uses the averaged-amplitude approach or not (there is no incoherent elastic scattering at forward angle in the form-factor approximation). As one moves away from forward angle there will be differences, but these valence-electron contributions are all decreasing rapidly compared to the contributions from the other electrons, so that any differences will be a small effect in the scattering cross section. Therefore for such elements and energies any corrections

associated with performing the more proper averaging over cross sections for the contribution of the valence electrons to the elastic coherent scattering, and including elastic incoherent scattering, should be small.

We expect that correct averaging, and inclusion of incoherent contributions, will matter most for low-Z elements, and in particular for excited atoms and ions, where many electrons are in partially filled subshells. In the next section we generalize the coherent Rayleigh scattering formalism, which used the averaged-amplitude approach, exact only for fully filled subshells, and describe elastic scattering from targets with partially filled subshells. This involves performing a more proper averaging over cross sections, including incoherent elastic scattering in which the initial and final atomic states are different, but energy degenerate. We also consider inelastic incoherent scattering between nearly energy-degenerate levels, which may become degenerate in a simpler theory or may not be resolved in energy in a realistic experimental situation. For completeness we also mention the available more general approaches for describing inelastic Raman and Compton scattering, which may be observed together with elastic scattering, depending on the energy resolution. In Sec. III we consider the example of elastic scattering from an excited hydrogen atom in the $2p$ state, and we recover the nonrelativistic elastic scattering cross section from the relativistic viewpoint. Implications for scattering from many-electron atoms are discussed in Sec. IV and conclusions are presented in Sec. V.

II. DESCRIPTIONS OF SCATTERING

Generally one is dealing with scattering from many-electron atoms, involving many-electron wave functions, and summations over the spatial coordinates of all the electrons in the expressions for the photon operators. However in independent-particle approximation one can reduce this many-electron problem to a single-electron formalism, in terms of single-electron scattering amplitudes corresponding to an electron making a transition from a definite initial state to a definite final state (which may or may not be the same state), through all possible intermediate states, regardless of their occupation [1]. In obtaining the total coherent amplitude, one should sum over the amplitudes for scattering from each electron of the atom. For incoherent scattering one sums instead cross sections for incoherent scattering from each electron of the atom.

In Sec. II A the formalism for calculating the single-electron scattering amplitudes is developed. Following this in Sec. II B we show how one then obtains the scattering cross sections for many-electron atoms, in accordance with Ref. [1]. In Sec. II C we perform a tensor decomposition of the elastic scattering cross section, giving separate explicit expressions for the coherent and incoherent elastic scattering cross section, and in Sec. II D we discuss consequences of energy resolution.

A. Single-electron scattering amplitudes

We now proceed to describe the evaluation of the single-electron scattering amplitudes in the second-order S-matrix approach, in which an atomic electron makes a transition from an initial state $|i\rangle=|n_i\kappa_i m_i\rangle$ with energy E_i to a final state $|f\rangle=|n_f\kappa_f m_f\rangle$ with energy E_f, which may or may not be the same state. The states are solutions of the Dirac equation in the presence of a self-consistent Dirac-Slater type central potential $V(r)$. The absorbed (emitted) photon has momentum $\boldsymbol{k}_a$ ($\boldsymbol{k}_e$) and polarization vector $\boldsymbol{\epsilon}_a$ ($\boldsymbol{\epsilon}_e$), and $k_a=|\boldsymbol{k}_a|=\omega_a/c$ ($k_e=|\boldsymbol{k}_e|=\omega_e/c$). The angle between the initial and final photon is θ and $\hat{\boldsymbol{k}}_a\cdot\hat{\boldsymbol{k}}_e=\cos\theta$. We use natural units $\hbar=m=c=1$ throughout. The relevant S-matrix element in the Furry representation is

$$S_{fi}=-2\pi i\,\delta(E_f+\omega_e-E_i-\omega_a)\sqrt{\frac{2\pi\alpha}{k_e}}\sqrt{\frac{2\pi\alpha}{k_a}}\mathcal{M}_{fi}, \tag{1}$$

where

$$\mathcal{M}_{fi}=\sum_n^{\mathcal{F}}\left(\frac{\langle f|A^*|n\rangle\langle n|A|i\rangle}{E_i+\omega_a-E_n}+\frac{\langle f|A|n\rangle\langle n|A^*|i\rangle}{E_i-\omega_e-E_n}\right), \tag{2}$$

and $A=\boldsymbol{\alpha}\cdot\boldsymbol{\epsilon}_a e^{i\boldsymbol{k}_a\cdot\boldsymbol{r}}$, $A^*=\boldsymbol{\alpha}\cdot\boldsymbol{\epsilon}_e^* e^{-i\boldsymbol{k}_e\cdot\boldsymbol{r}}$ are the photon absorption and emission operators, respectively. The summation/integration is over all intermediate states $|n\rangle$ (both bound and in the continuum) in the atomic potential $V(r)$.

We perform a multipole expansion of both photon operators:

$$\begin{aligned}A&=\sum_{J_aM_a\lambda_a}C^{\lambda_a}_{J_aM_a}(\hat{\boldsymbol{k}}_a,\boldsymbol{\epsilon}_a)A^{\lambda_a}_{J_aM_a}(k_ar),\\ A^*&=\sum_{J_eM_e\lambda_e}C^{\lambda_e*}_{J_eM_e}(\hat{\boldsymbol{k}}_e,\boldsymbol{\epsilon}_e)A^{\lambda_e*}_{J_eM_e}(k_er).\end{aligned} \tag{3}$$

The definitions of $C^{\lambda}_{JM}(\hat{\boldsymbol{k}},\boldsymbol{\epsilon})$ and $A^{\lambda}_{JM}(kr)$ are given in Appendix A. We choose a coordinate system in which the z axis is directed along the direction of the incident photon $\hat{\boldsymbol{z}}=\hat{\boldsymbol{k}}_a$. Now we can write the scattering amplitude as

$$\mathcal{M}_{fi}=\sum_{J_aM_a\lambda_a}\sum_{J_eM_e\lambda_e}C^{\lambda_a}_{J_aM_a}(\hat{\boldsymbol{k}}_a,\boldsymbol{\epsilon}_a)C^{\lambda_e*}_{J_eM_e}(\hat{\boldsymbol{k}}_e,\boldsymbol{\epsilon}_e)M^{J_e,M_e,\lambda_e}_{J_a,M_a,\lambda_a}, \tag{4}$$

where

$$M^{J_e,M_e,\lambda_e}_{J_a,M_a,\lambda_a}=\sum_n^{\mathcal{F}}\left(\frac{\langle f|A^{\lambda_e*}_{J_eM_e}(k_er)|n\rangle\langle n|A^{\lambda_a}_{J_aM_a}(k_ar)|i\rangle}{E_i+\omega_a-E_n}+\frac{\langle f|A^{\lambda_a}_{J_aM_a}(k_ar)|n\rangle\langle n|A^{\lambda_e*}_{J_eM_e}(k_er)|i\rangle}{E_i-\omega_e-E_n}\right). \tag{5}$$

The quantity $C^{\lambda_a}_{J_aM_a}(\hat{\boldsymbol{k}}_a,\boldsymbol{\epsilon}_a)C^{\lambda_e*}_{J_eM_e}(\hat{\boldsymbol{k}}_e,\boldsymbol{\epsilon}_e)$ depends only on the scattering angle θ and the polarization vectors, whereas the quantity $M^{J_e,M_e,\lambda_e}_{J_a,M_a,\lambda_a}$ depends the photon energies and contains all the atomic information.

As was done for the coherent Rayleigh scattering amplitude [2,4,5], we write Eq. (5) in the form

$$M^{J_e,M_e,\lambda_e}_{J_a,M_a,\lambda_a} = \langle f|A^{\lambda_e *}_{J_eM_e}(k_e r)|i+\rangle^{\lambda_a}_{J_aM_a} + \langle f|A^{\lambda_a}_{J_aM_a}(k_a r)|i-\rangle^{\lambda_e}_{J_eM_e}, \tag{6}$$

where we have defined the positive frequency

$$|i+\rangle^{\lambda_a}_{J_aM_a} = |n_i\kappa_i m_i+\rangle^{\lambda_a}_{J_aM_a} = \sum\!\!\!\!\!\!\int_n \frac{|n\rangle\langle n|A^{\lambda_a}_{J_aM_a}(k_a r)|n_i\kappa_i m_i\rangle}{E_i+\omega_a-E_n}, \tag{7}$$

and negative frequency

$$|i-\rangle^{\lambda_e}_{J_eM_e} = |n_i\kappa_i m_i-\rangle^{\lambda_e}_{J_eM_e} = \sum\!\!\!\!\!\!\int_n \frac{|n\rangle\langle n|A^{\lambda_e *}_{J_eM_e}(k_e r)|n_i\kappa_i m_i\rangle}{E_i-\omega_e-E_n}, \tag{8}$$

perturbed orbitals which satisfy the following inhomogeneous Dirac equations (H is the Hamiltonian):

$$\begin{aligned}(E_i+\omega_a-H)|n_i\kappa_i m_i+\rangle^{\lambda_a}_{J_aM_a} &= A^{\lambda_a}_{J_aM_a}(k_a r)|n_i\kappa_i m_i\rangle,\\ (E_i-\omega_e-H)|n_i\kappa_i m_i-\rangle^{\lambda_e}_{J_eM_e} &= A^{\lambda_e *}_{J_eM_e}(k_e r)|n_i\kappa_i m_i\rangle.\end{aligned} \tag{9}$$

These are still three-dimensional equations, and we need to expand both sides of Eq. (9) in a spherical basis to obtain the radial differential equations that will be solved numerically.

We consider the action of the photon operator $A^{\lambda}_{JM}(kr)$ on a state $|n\kappa m\rangle$, giving the result in a spherical basis (as was done in Refs. [3,5], see also Ref. [29] for details)

$$A^{\lambda=1}_{JM}(kr)|n\kappa m\rangle = \sum_{\kappa' m'} i\frac{\sqrt{J(J+1)}}{2J+1} I^{JM}_{\kappa' m',\kappa m}\frac{1}{r} \times \begin{pmatrix} K^{\lambda=1}_{\kappa' Jn\kappa}(k,r)\Omega_{\kappa' m'}(\hat{\mathbf{r}}) \\ iL^{\lambda=1}_{\kappa' Jn\kappa}(k,r)\Omega_{-\kappa' m'}(\hat{\mathbf{r}}) \end{pmatrix}, \tag{10}$$

$$A^{\lambda=0}_{JM}(kr)|n\kappa m\rangle = \sum_{\kappa' m'} -i\frac{(\kappa'+\kappa)}{\sqrt{J(J+1)}} I^{JM}_{-\kappa' m',\kappa m}\frac{1}{r} \times \begin{pmatrix} K^{\lambda=0}_{\kappa' Jn\kappa}(k,r)\Omega_{\kappa' m'}(\hat{\mathbf{r}}) \\ iL^{\lambda=0}_{\kappa' Jn\kappa}(k,r)\Omega_{-\kappa' m'}(\hat{\mathbf{r}}) \end{pmatrix},$$

where the angular integral $I^{JM}_{\kappa' m',\kappa m}$ is defined in Appendix B, and we have defined

$$\begin{pmatrix} K^{\lambda=0}_{\kappa' Jn\kappa}(k,r) \\ L^{\lambda=0}_{\kappa' Jn\kappa}(k,r) \end{pmatrix} = \begin{pmatrix} j_J(kr)f_{n\kappa}(r) \\ j_J(kr)g_{n\kappa}(r) \end{pmatrix},$$

$$\begin{pmatrix} K^{\lambda=1}_{\kappa' Jn\kappa}(k,r) \\ L^{\lambda=1}_{\kappa' Jn\kappa}(k,r) \end{pmatrix} = \begin{pmatrix} \left[\left(\frac{\kappa'-\kappa-J}{J}\right)j_{J-1}(kr) - \left(\frac{\kappa'-\kappa+J+1}{J+1}\right)j_{J+1}(kr)\right]f_{n\kappa}(r) \\ \left[\left(\frac{\kappa'-\kappa+J}{J}\right)j_{J-1}(kr) - \left(\frac{\kappa'-\kappa-J-1}{J+1}\right)j_{J+1}(kr)\right]g_{n\kappa}(r) \end{pmatrix}, \tag{11}$$

where $j_J(kr)$ is the spherical Bessel function of order J with argument kr. The corresponding expansions for $A^{\lambda *}_{JM}(kr)|n\kappa m\rangle$ are obtained by the substitution $M\to -M$ and including a factor $(-1)^M$, which follows from the properties of the spherical harmonic Y_{JM}.

Now we expand the perturbed orbitals in the spherical basis in the same way as we expand the driving terms of the inhomogeneous equations [right-hand side of Eq. (9)], giving for the positive frequency perturbed orbital

$$|n_i\kappa_i m_i+\rangle^{\lambda_a=1}_{J_aM_a} = \sum_{\kappa' m'} i\frac{\sqrt{J_a(J_a+1)}}{2J_a+1} I^{J_aM_a}_{\kappa' m',\kappa_i m_i}\frac{1}{r} \times \begin{pmatrix} S^{(+)\lambda_a=1}_{\kappa' J_a n_i\kappa_i}(k_a,r)\Omega_{\kappa' m'}(\hat{\mathbf{r}}) \\ iT^{(+)\lambda_a=1}_{\kappa' J_a n_i\kappa_i}(k_a,r)\Omega_{-\kappa' m'}(\hat{\mathbf{r}}) \end{pmatrix}, \tag{12}$$

$$|n_i\kappa_i m_i+\rangle^{\lambda_a=0}_{J_aM_a}=\sum_{\kappa' m'} -i\frac{(\kappa'+\kappa_i)}{\sqrt{J_a(J_a+1)}}I^{J_aM_a}_{-\kappa' m',\kappa_i m_i}\frac{1}{r}\times\begin{pmatrix} S^{(+)\lambda_a=0}_{\kappa' J_a n_i\kappa_i}(k_a,r)\Omega_{\kappa' m'}(\hat{\mathbf{r}}) \\ iT^{(+)\lambda_a=0}_{\kappa' J_a n_i\kappa_i}(k_a,r)\Omega_{-\kappa' m'}(\hat{\mathbf{r}})\end{pmatrix},$$

and similarly for the negative frequency perturbed orbital

$$|n_i\kappa_i m_i-\rangle^{\lambda_e=1}_{J_eM_e}=\sum_{\kappa' m'} i\frac{\sqrt{J_e(J_e+1)}}{2J_e+1}I^{J_eM_e}_{\kappa' m',\kappa_i m_i}\frac{1}{r}\times\begin{pmatrix} S^{(-)\lambda_e=1}_{\kappa' J_e n_i\kappa_i}(k_e,r)\Omega_{\kappa' m'}(\hat{\mathbf{r}}) \\ iT^{(-)\lambda_e=1}_{\kappa' J_e n_i\kappa_i}(k_e,r)\Omega_{-\kappa' m'}(\hat{\mathbf{r}})\end{pmatrix},$$

$$|n_i\kappa_i m_i-\rangle^{\lambda_e=0}_{J_eM_e}=\sum_{\kappa' m'} -i\frac{(\kappa'+\kappa_i)}{\sqrt{J_e(J_e+1)}}I^{J_eM_e}_{-\kappa' m',\kappa_i m_i}\frac{1}{r}\times\begin{pmatrix} S^{(-)\lambda_e=0}_{\kappa' J_e n_i\kappa_i}(k_e,r)\Omega_{\kappa' m'}(\hat{\mathbf{r}}) \\ iT^{(-)\lambda_e=0}_{\kappa' J_e n_i\kappa_i}(k_e,r)\Omega_{-\kappa' m'}(\hat{\mathbf{r}})\end{pmatrix}. \tag{13}$$

With this decomposition Eq. (9) leads to the functions $S^{(+)\lambda_a}_{\kappa' J_a n_i\kappa_i}(k_a,r)$ and $T^{(+)\lambda_a}_{\kappa' J_a n_i\kappa_i}(k_a,r)$ satisfying the following radial differential equations:

$$\begin{aligned}&[E_i+\omega_a-1-V(r)]S^{(+)\lambda_a}_{\kappa' J_a n_i\kappa_i}(k_a,r)+\left(\frac{d}{dr}-\frac{\kappa'}{r}\right)T^{(+)\lambda_a}_{\kappa' J_a n_i\kappa_i}(k_a,r)=K^{\lambda_a}_{\kappa' J_a n_i\kappa_i}(k_a,r),\\ &[E_i+\omega_a+1-V(r)]T^{(+)\lambda_a}_{\kappa' J_a n_i\kappa_i}(k_a,r)-\left(\frac{d}{dr}+\frac{\kappa'}{r}\right)S^{(+)\lambda_a}_{\kappa' J_a n_i\kappa_i}(k_a,r)=L^{\lambda_a}_{\kappa' J_a n_i\kappa_i}(k_a,r),\end{aligned} \tag{14}$$

while $S^{(-)\lambda_e}_{\kappa' J_e n_i\kappa_i}(k_e,r)$ and $T^{(-)\lambda_e}_{\kappa' J_e n_i\kappa_i}(k_e,r)$ satisfy

$$\begin{aligned}&[E_i-\omega_e-1-V(r)]S^{(-)\lambda_e}_{\kappa' J_e n_i\kappa_i}(k_e,r)+\left(\frac{d}{dr}-\frac{\kappa'}{r}\right)T^{(-)\lambda_e}_{\kappa' J_e n_i\kappa_i}(k_e,r)=K^{\lambda_e}_{\kappa' J_e n_i\kappa_i}(k_e,r),\\ &[E_i-\omega_e+1-V(r)]T^{(-)\lambda_e}_{\kappa' J_e n_i\kappa_i}(k_e,r)-\left(\frac{d}{dr}+\frac{\kappa'}{r}\right)S^{(-)\lambda_e}_{\kappa' J_e n_i\kappa_i}(k_e,r)=L^{\lambda_e}_{\kappa' J_e n_i\kappa_i}(k_e,r).\end{aligned} \tag{15}$$

The absorption first and emission first radial integrals that encompass all the dynamic and atomic information regarding scattering are, respectively,

$$\begin{aligned}R^{(+)\lambda_a\lambda_e}_{\kappa' J_a J_e}&=\int_0^\infty [K^{\lambda_e}_{\kappa' J_e n_f\kappa_f}(k_e,r)S^{(+)\lambda_a}_{\kappa' J_a n_i\kappa_i}(k_a,r)+L^{\lambda_e}_{\kappa' J_e n_f\kappa_f}(k_e,r)T^{(+)\lambda_a}_{\kappa' J_a n_i\kappa_i}(k_a,r)]dr,\\ R^{(-)\lambda_a\lambda_e}_{\kappa' J_a J_e}&=\int_0^\infty [K^{\lambda_a}_{\kappa' J_a n_f\kappa_f}(k_a,r)S^{(-)\lambda_e}_{\kappa' J_e n_i\kappa_i}(k_e,r)+L^{\lambda_a}_{\kappa' J_a n_f\kappa_f}(k_a,r)T^{(-)\lambda_e}_{\kappa' J_e n_i\kappa_i}(k_e,r)]dr,\end{aligned} \tag{16}$$

where we have suppressed the implied indices $n_i\kappa_i, n_f\kappa_f$, related to the initial and final atomic states, and the arguments, k_a, k_e, r, on the left-hand side of Eq. (16) to avoid clutter.

In terms of these radial integrals, $M^{J_e,M_e,\lambda_e}_{J_a,M_a,\lambda_a}$ becomes

$$
\begin{aligned}
M^{J_e,M_e,\lambda_e=1}_{J_a,M_a,\lambda_a=1} &= \sum_{\kappa' m'} \frac{\sqrt{J_a(J_a+1)J_e(J_e+1)}}{(2J_a+1)(2J_e+1)} \Big[I^{J_a M_a}_{\kappa' m',\kappa_i m_i} I^{J_e M_e}_{\kappa' m',\kappa_f m_f} R^{(+)11}_{\kappa' J_a J_e} \\
&\quad + (-1)^{(M_a+M_e)} I^{J_e - M_e}_{\kappa' m',\kappa_i m_i} I^{J_a - M_a}_{\kappa' m',\kappa_f m_f} R^{(-)11}_{\kappa' J_a J_e} \Big], \\
M^{J_e,M_e,\lambda_e=0}_{J_a,M_a,\lambda_a=0} &= \sum_{\kappa' m'} \frac{(\kappa'+\kappa_i)(\kappa'+\kappa_f)}{\sqrt{J_a(J_a+1)J_e(J_e+1)}} \Big[I^{J_a M_a}_{-\kappa' m',\kappa_i m_i} I^{J_e M_e}_{-\kappa' m',\kappa_f m_f} R^{(+)00}_{\kappa' J_a J_e} \\
&\quad + (-1)^{(M_a+M_e)} I^{J_e - M_e}_{-\kappa' m',\kappa_i m_i} I^{J_a - M_a}_{-\kappa' m',\kappa_f m_f} R^{(-)00}_{\kappa' J_a J_e} \Big], \\
M^{J_e,M_e,\lambda_e=0}_{J_a,M_a,\lambda_a=1} &= \sum_{\kappa' m'} -\frac{\sqrt{J_a(J_a+1)}}{(2J_a+1)\sqrt{J_e(J_e+1)}} \Big[(\kappa'+\kappa_f) \\
&\quad \times I^{J_a M_a}_{\kappa' m',\kappa_i m_i} I^{J_e M_e}_{-\kappa' m',\kappa_f m_f} R^{(+)10}_{\kappa' J_a J_e} \\
&\quad + (-1)^{(M_a+M_e)} (\kappa'+\kappa_i) I^{J_e - M_e}_{-\kappa' m',\kappa_i m_i} \\
&\quad \times I^{J_a - M_a}_{\kappa' m',\kappa_f m_f} R^{(-)10}_{\kappa' J_a J_e} \Big], \\
M^{J_e,M_e,\lambda_e=1}_{J_a,M_a,\lambda_a=0} &= \sum_{\kappa' m'} -\frac{\sqrt{J_e(J_e+1)}}{(2J_e+1)\sqrt{J_a(J_a+1)}} \Big[(\kappa'+\kappa_i) \\
&\quad \times I^{J_a M_a}_{-\kappa' m',\kappa_i m_i} I^{J_e M_e}_{\kappa' m',\kappa_f m_f} R^{(+)01}_{\kappa' J_a J_e} \\
&\quad + (-1)^{(M_a+M_e)} (\kappa'+\kappa_f) I^{J_e - M_e}_{\kappa' m',\kappa_i m_i} \\
&\quad \times I^{J_a - M_a}_{-\kappa' m',\kappa_f m_f} R^{(-)01}_{\kappa' J_a J_e} \Big].
\end{aligned}
\tag{17}
$$

The results in Eq. (17) give the amplitude in terms of definite radial integrals that, together with explicit expressions for $C^{\lambda}_{J_a M_a}(\hat{\boldsymbol{k}}_a) C^{\lambda *}_{J_e M_e}(\hat{\boldsymbol{k}}_e)$, allow the calculation of the single-electron scattering amplitude corresponding to an electron making a transition from an initial state $|n_i \kappa_i m_i\rangle$ to a final state $|n_f \kappa_f m_f\rangle$, which may or may not be the same state.

B. Whole-atom cross sections

For a given many-electron atomic configuration (with definite magnetic substate occupations) one obtains the whole-atom elastic coherent scattering amplitude by coherently summing all the single-electron scattering amplitudes, as well as other coherent amplitudes such as the nuclear Thomson amplitude as appropriate (as described in Ref. [1]). For the case of a single partially filled subshell (the results are easily generalized to many subshells), we denote by I the set of occupied magnetic substates in the subshell (thus specifying the state of the atom completely), and by $\overline{I}$ the complementary set of unoccupied magnetic substates. The coherent elastic cross section for the configuration I is

$$
\frac{d\sigma^I}{d\Omega_{\text{coherent}}} = \left| \sum_{i \in I} \mathcal{M}_{ii} + A_{\text{other}} \right|^2, \tag{18}
$$

where A_{other} represent other coherent contributions, such as the coherent nuclear Thomson amplitude. The incoherent elastic scattering cross section for the configuration I is

$$
\frac{d\sigma^I}{d\Omega_{\text{incoherent}}} = \sum_{i \in I, f \in \overline{I}} |\mathcal{M}_{fi}|^2, \tag{19}
$$

corresponding to the sum of cross sections for single-electron transitions to the unoccupied substates $\overline{I}$, where we are summing over possible final configurations $I' = I - i + f$.

The inelastic incoherent cross section corresponding to the inelastic transitions to the set of unoccupied substates $\overline{J}$ of another subshell (Raman scattering) is

$$
\frac{d\sigma^{I\overline{J}}}{d\Omega_{\text{inelastic}}} = \sum_{i \in I, f \in \overline{J}} \frac{\omega_e}{\omega_a} |\mathcal{M}_{fi}|^2, \tag{20}
$$

where ω_a (ω_e) is the incident (scattered) photon energy. Energy resolution will determine which other subshells should be considered.

In choosing definite integral magnetic substate occupations for each of the electrons in partially filled subshells (and then averaging over the possibilities) we are not generally dealing with eigenstates of total angular momentum of the atom as a whole. Since we are interested in scattering cross sections for randomly oriented targets, where each substate in a given subshell has equal weight (rather than dealing with observed initial and final states of definite total angular momentum and projection), this is equivalent to using and averaging over the allowed eigenstates of total angular momentum in getting the randomly oriented cross section for specified numbers of electrons in each subshell. Of course, if one instead wanted to consider scattering in which the initial or final total angular momentum of the atom was observed, these states would have to be explicitly constructed. This would be necessary for describing magnetic scattering, when the target has a definite orientation, for which there are experiments [30].

Here we consider the case of scattering from a randomly-oriented target with final target orientations not being observed. One should average over initial target orientations and sum over all final target orientations. This corresponds to averaging the above cross sections over all possible initial magnetic substate occupations I for a given situation. For example, if we have a $p_{3/2}$ subshell (with four magnetic substates corresponding to $m=-3/2,-1/2,+1/2,+3/2$) with 2 electrons present there are six possible magnetic substate occupations

$$I=\left(-\frac{3}{2},-\frac{1}{2}\right),\left(-\frac{3}{2},+\frac{1}{2}\right),\left(-\frac{3}{2},+\frac{3}{2}\right),\left(-\frac{1}{2},+\frac{1}{2}\right),$$

$$\left(-\frac{1}{2},+\frac{3}{2}\right),\left(+\frac{1}{2},+\frac{3}{2}\right), \tag{21}$$

and the cross sections should be averaged over the different choices for I. For incoherent elastic scattering Eq. (19) has already summed cross sections over final state configurations I'.

In the averaged-amplitude approach (exact for elastic scattering from closed shells) one considers only elastic coherent scattering (so the initial and final states are the same, $|n_i\kappa_i m_i\rangle=|n_f\kappa_f m_f\rangle$, and the photon energies are the same, $k_a=k_e$). One sums the amplitude over all magnetic substates and finally weights the amplitude according to the number of electrons actually present in the subshell. This corresponds to taking the weighted summation $[N_e/(2j_i+1)]\Sigma_{m_i m_f}\delta_{n_i,n_f}\delta_{\kappa_i,\kappa_f}\delta_{m_i,m_f}$ over the single-electron scattering amplitude $\mathcal{M}_{fi}$, where N_e is the number of electrons actually present in the subshell. A consequence is that only the diagonal terms in the cross product of the multipole expansions of the two photon operators survive. Taking $J_aM_a\lambda_a=J_eM_e\lambda_e=JM\lambda$, $n_i\kappa_i m_i=n_f\kappa_f m_f=n\kappa m$, and $k_a=k_e=k$ allows us to write the averaged-amplitude result (which is squared to give the elastic scattering cross section) as

$$\mathcal{M}_{\text{ave amp}}=\frac{N_e}{2j_i+1}\sum_{JM\lambda} C^{\lambda}_{JM}(\hat{\boldsymbol{k}}_a)C^{\lambda *}_{JM}(\hat{\boldsymbol{k}}_e)M_{J,\lambda}, \tag{22}$$

where $C^{\lambda}_{JM}(\hat{\boldsymbol{k}}_a)C^{\lambda *}_{JM}(\hat{\boldsymbol{k}}_e)$ is given explicitly in Appendix A and

$$M_{J,\lambda=1}=\frac{(2j+1)}{4\pi}\sum_{\kappa'}\Pi_{lJl'}C^2\left(jJj';\frac{1}{2}0\frac{1}{2}\right)\frac{J(J+1)}{(2J+1)^2}$$
$$\times[R^{(+)11}_{\kappa' JJ}+R^{(-)11}_{\kappa' JJ}], \tag{23}$$

$$M_{J,\lambda=0}=\frac{(2j+1)}{4\pi}\sum_{\kappa'}\Pi_{lJ\bar{l}'}C^2\left(jJj';\frac{1}{2}0\frac{1}{2}\right)\frac{(\kappa'+\kappa)^2}{J(J+1)}$$
$$\times[R^{(+)00}_{\kappa' JJ}+R^{(-)00}_{\kappa' JJ}].$$

(In the above l' corresponds to the orbital angular momentum eigenvalue of the large component of the total angular momentum eigenstate specified by the Dirac quantum number κ', while $\bar{l}'$ denotes the corresponding eigenvalue for $-\kappa'$.) Note here that the scattering cross section depends only on the sum of corresponding positive and negative frequency radial integrals (rather than each separately), whereas this is not true in general. Part of the attraction of using the averaged-amplitude approach is the simplification that occurs—only the diagonal elements in the products of the multipole expansion of the two photon operators survive, and this reduces the number of radial integrals that have to be calculated. These calculations are intensive, since for x-ray and γ-ray energies one often needs to calculate many multipoles to get convergence (as high as $J=100$ not being unusual).

It is not necessary to proceed to the full evaluation of all multipoles (up to the highest multipole needed for overall convergence) for each subshell in order to estimate the correction associated with going beyond the averaged-amplitude result. It is well known that one can describe Rayleigh scattering using modified form factors and angle-independent anomalous scattering factors (MFF+ASF), obtaining results in good agreement with the S-matrix results [8]. [This is not the case for large-angle scattering for high-Z elements for photon energies above the innershell thresholds, but since the amplitude is dominated in this case by the innershell (fully filled for high-Z ground-state atoms) ASF, we do not expect large corrections to the averaged-amplitude result here.] The agreement of (MFF+ASF) with the S-matrix results indicates that the part of the full amplitude corresponding to the ASF at forward angle is dominated by the leading electric dipole multipole (which gives an angle-independent ASF), while the MFF part will involve higher multipoles, and it falls off more quickly with increasing angle [10,11]. Therefore one can obtain the correction to the averaged-amplitude approach by evaluating the modified form factor, performing the proper averaging, and taking the beyond-form-factor correction at the electric dipole level. Inner shells may be completely described at the electric dipole level, while outer shells may be completely described in the form-factor approximation, depending on the photon energy. (Note that the

correction vanishes at the form-factor level for forward angle, and the electric dipole corrections for the form factor vanish in the long wavelength limit, since in both cases the interaction operator $A^2 \to 1$.)

C. Tensor decomposition of elastic cross sections

The scattering amplitude can be written in terms of a sum over the direct tensor product of the photon multipoles, which are themselves spherical tensors [see Eq. (A1)], or in terms of a sum of irreducible tensor amplitudes of fixed rank. The coefficients (involving the photon polarizations and the scattering angle) will have tensor character also, as the scattering amplitude must be a scalar. Further, one can show that the cross section for elastic scattering from randomly oriented targets separates into a sum of positive components, each being a partial cross section associated with one of the irreducible tensor amplitudes, i.e., there are no cross terms between the irreducible tensor amplitudes in the randomly oriented cross section [31]. This is well known in nonrelativistic dipole approximation, where the amplitude, involving the direct product of two dipole operators (of rank 1), can be written as a sum over irreducible tensor amplitudes of ranks 0, 1, and 2. The randomly oriented scattering cross section in that case therefore separates into partial cross sections associated with the irreducible tensor amplitudes of ranks 0, 1, and 2 [29,32]. The partial cross section associated with the irreducible tensor amplitude of rank 0 is often referred to as the scalar scattering cross section, referring to the fact that the corresponding irreducible tensor amplitude is itself a scalar (as is its coefficient).

In fact the averaged-amplitude result corresponds exactly to the scalar partial cross section, which is entirely coherent (since, due to the scalar character of the product of photon multipoles, transitions to different substates are forbidden, leaving the state unchanged). Effects beyond the averaged-amplitude result are due to partial cross sections of higher rank, which include both coherent and incoherent components.

We illustrate this decomposition of the full expansion in multipoles, considering first the single-particle case in which the initial (final) angular momentum of the particle and its projection is j_i, m_i (j_f, m_f). The use of recoupling rules for irreducible tensors allows us to express Eq. (4) in the form

$$\mathcal{M}_{fi} = \sqrt{2j_i+1}(-1)^{j_i-m_i} \sum_{p=|j_i-j_f|}^{j_i+j_f} C(j_i j_f p; m_i - m_f \mu) \times \sum_{J_a,J_e=0}^{\infty} \sum_{\lambda_a,\lambda_e=0}^{1} T^{J_a\lambda_a;J_e\lambda_e}_{p-\mu}(\boldsymbol{\epsilon}_a, \boldsymbol{\epsilon}_e^*)\, \alpha^{\lambda_a\lambda_e}_{pJ_aJ_e}(k_a, k_e), \tag{24}$$

where

$$T^{J_a\lambda_a;J_e\lambda_e}_{p\mu}(\boldsymbol{\epsilon}_a, \boldsymbol{\epsilon}_e^*) = 4\pi\{(\mathbf{Y}^{(\lambda_a)}_{J_a}(\hat{\boldsymbol{k}}_a)\cdot\boldsymbol{\epsilon}_a)\otimes(\mathbf{Y}^{(\lambda_e)}_{J_e}(\hat{\boldsymbol{k}}_e)\cdot\boldsymbol{\epsilon}_e^*)\}_{p\mu}, \tag{25}$$

in terms of vector spherical harmonics. Here the angle-independent atomic parameters are

$$\begin{aligned}\alpha^{\lambda_a\lambda_e}_{pJ_aJ_e}(k_a,k_e) = {} & (i)^{J_a+\lambda_a-J_e+\lambda_e}\sqrt{2j_f+1}\left[\frac{J_a(J_a+1)}{2J_a+1}\right]^{\lambda_a-1/2} \\ & \times\left[\frac{J_e(J_e+1)}{2J_e+1}\right]^{\lambda_e-1/2}\sum_{\kappa'}(-1)^{j'-j_f} \\ & \times\left(C\left(j_iJ_aj';\frac{1}{2}0\frac{1}{2}\right)C\left(j_fJ_ej';\frac{1}{2}0\frac{1}{2}\right)\right. \\ & \times\begin{Bmatrix} J_e & J_a & p \\ j_i & j_f & j'\end{Bmatrix} B^{(+)}_{\kappa'\lambda_a\lambda_e} R^{(+)\lambda_a\lambda_e}_{\kappa' J_aJ_e} \\ & +(-1)^{p+J_a+J_e}C\left(j_iJ_ej';\frac{1}{2}0\frac{1}{2}\right) \\ & \times C\left(j_fJ_aj';\frac{1}{2}0\frac{1}{2}\right) \\ & \left.\times\begin{Bmatrix} J_e & J_a & p \\ j_f & j_i & j'\end{Bmatrix} B^{(-)}_{\kappa'\lambda_a\lambda_e} R^{(-)\lambda_a\lambda_e}_{\kappa' J_aJ_e}\right),\end{aligned} \tag{26}$$

involving the Wigner 6-j symbol, the Clebsch-Gordon coefficients, and

$$\begin{aligned} & B^{(+)}_{\kappa' 11} = \Pi_{l' J_a l_i}, \quad B^{(-)}_{\kappa' 11} = \Pi_{l' J_e l_i}, \\ & B^{(+)}_{\kappa' 00} = (\kappa'+\kappa_i)(\kappa'+\kappa_f)\Pi_{\bar{l}' J_a l_i}, \\ & B^{(-)}_{\kappa' 00} = (\kappa'+\kappa_i)(\kappa'+\kappa_f)\Pi_{\bar{l}' J_e l_i}, \\ & B^{(+)}_{\kappa' 10} = (\kappa'+\kappa_f)\Pi_{l' J_a l_i}, \quad B^{(-)}_{\kappa' 10} = (\kappa'+\kappa_i)\Pi_{\bar{l}' J_e l_i}, \\ & B^{(+)}_{\kappa' 01} = (\kappa'+\kappa_i)\Pi_{\bar{l}' J_a l_i}, \quad B^{(-)}_{\kappa' 01} = (\kappa'+\kappa_f)\Pi_{l' J_e l_i}, \end{aligned} \tag{27}$$

where $\Pi_{l' J_a l_i} = 1$ if $l' + J_a + l_i$ is an even number, and it is zero otherwise; $\bar{l}' = l(-\kappa')$. As a consequence of parity conservation, $J_a + J_e + \lambda_a + \lambda_e + l_i + l_f$ is an even number (l_i, l_f denote initial and final parities, respectively). In the averaged-amplitude approach only the terms with $p = 0$ in Eq. (24) survive. (This case, together with the special case of $j_i = j_f = 1/2$, $l_i = l_f$, is discussed in detail in Ref. [31].)

Now let us consider the case of elastic scattering by an atom with one closed shell occupied by $2j_c+1$ electrons with quantum numbers n_c, κ_c, and one partially filled subshell occupied by N_e electrons with quantum numbers n_i, κ_i ($N_e \leqslant N_t$, where $N_t = 2j_i + 1$ is the number of different one-electron magnetic substates in the partially filled subshell).

In accordance with Eq. (24), the amplitude of the coherent scattering is

$$\mathcal{A}_{\rm coh}=\sum_{J_a,J_e=0}^{\infty}\sum_{\lambda_a,\lambda_e=0}^{1}\left(\sqrt{2j_i+1}\sum_{m_i\in I}\sum_{p=0}^{2j_i}(-1)^{j_i-m_i}\times C(j_ij_ip;m_i-m_i0)T_{p-\mu}^{J_a\lambda_a;J_e\lambda_e}(\boldsymbol{\epsilon}_a,\boldsymbol{\epsilon}_e^*)\alpha_{pJ_aJ_e}^{\lambda_a\lambda_e}(n_i,\kappa_i)+(2j_c+1)T_{00}^{J_a\lambda_a;J_a\lambda_a}(\boldsymbol{\epsilon}_a,\boldsymbol{\epsilon}_e^*)\alpha_{pJ_aJ_a}^{\lambda_a\lambda_a}(n_c,\kappa_c)\right),\quad(28)$$

where I is the set of occupied magnetic substates in the subshell, the radial parameters $\alpha_{pJ_aJ_e}^{\lambda_a\lambda_e}(n,\kappa)$ correspond to one-electron transitions within the level with quantum numbers n, κ [defined by Eq. (26)], and $k_a=k_e$.

The amplitude of incoherent elastic scattering has the form

$$\mathcal{A}_{\rm incoh}=\sqrt{2j_i+1}\sum_{J_a,J_e=0}^{\infty}\sum_{\lambda_a,\lambda_e=0}^{1}\sum_{p=0}^{2j_i}(-1)^{j_i-m_i}\times C(j_ij_ip;m_i-m_f\mu)T_{p-\mu}^{J_a\lambda_a;J_e\lambda_e}(\boldsymbol{\epsilon}_a,\boldsymbol{\epsilon}_e^*)\times\alpha_{pJ_aJ_e}^{\lambda_a\lambda_e}(n_i,\kappa_i),\quad m_i\in I,\quad m_f\notin I.\quad(29)$$

We see that only the partially-filled subshell contributes to the incoherent elastic amplitude.

As was mentioned above, the elastic scattering cross section is a sum of terms corresponding to the coherent and incoherent scattering summed over final and averaged over initial magnetic substate occupations. This leads to the appearance of the factor $\binom{N_t}{N_e}^{-1}$ [$\binom{a}{b}$ is the binomial coefficient] in the expression for the cross section

$$\frac{d\sigma}{d\Omega}=\binom{N_t}{N_e}^{-1}\sum_I\left(|\mathcal{A}_{\rm coh.}|^2+\sum_{m_i\in I,m_f\notin I}|\mathcal{A}_{\rm incoh}|^2\right).\quad(30)$$

The ''incoherent part'' of the cross section can be written in the form

$$\sum_I\sum_{m_i\in I,m_f\notin I}|\mathcal{A}_{\rm incoh}|^2=N_t\binom{N_t-2}{N_e-1}\sum_{p=1}^{N_t-1}\sum_{(J)=0}^{\infty}\sum_{(\lambda)=0}^{1}\alpha_{pJ_aJ_e}^{\lambda_a\lambda_e}(n_i,\kappa_i)\alpha_{pJ_a'J_e'}^{\lambda_a'\lambda_e'}(n_i,\kappa_i)^*\times\sum_{\mu\neq0}T_{p-\mu}^{J_a\lambda_a;J_e\lambda_e}(\boldsymbol{\epsilon}_a,\boldsymbol{\epsilon}_e^*)T_{p-\mu}^{J_a'\lambda_a';J_e'\lambda_e'}(\boldsymbol{\epsilon}_a,\boldsymbol{\epsilon}_e^*)^*,\quad(31)$$

where summations are performed over all indices $(J)=(J_a,J_a',J_e,J_e')$, $(\lambda)=(\lambda_a,\lambda_a',\lambda_e,\lambda_e')$. Similarly, for the coherent part of the cross section

$$\sum_I|\mathcal{A}_{\rm coh.}|^2=\sum_{p=0}^{N_t-1}\sum_{(J)=0}^{\infty}\sum_{(\lambda)=0}^{1}T_{p0}^{J_a\lambda_a;J_e\lambda_e}(\boldsymbol{\epsilon}_a,\boldsymbol{\epsilon}_e^*)T_{p0}^{J_a'\lambda_a';J_e'\lambda_e'}(\boldsymbol{\epsilon}_a,\boldsymbol{\epsilon}_e^*)^*\Bigg\{\delta_{p,0}\binom{N_t}{N_e}\times[(N_e\alpha_{0J_aJ_a}^{\lambda_a\lambda_a}(n_i,\kappa_i)+(2j_c+1)\alpha_{0J_aJ_a}^{\lambda_a\lambda_a}(n_c,\kappa_c))(\text{same with } J_a,\lambda_a\to J_a',\lambda_a')^*]+(1-\delta_{p,0})N_t\binom{N_t-2}{N_e-1}\alpha_{pJ_aJ_e}^{\lambda_a\lambda_e}(n_i,\kappa_i)\alpha_{pJ_a'J_e'}^{\lambda_a'\lambda_e'}(n_i,\kappa_i)^*\Bigg\}.\quad(32)$$

After averaging over incident photon polarizations and summing over final photon polarizations, the cross section finally can be written in the form

$$\frac{d\sigma}{d\Omega}=\frac{1}{4\pi}\sum_{c=0}^{\infty}P_c(\cos\theta)\sigma_c,\quad(33)$$

where σ_0 is the total cross-section, integrated over scattered photon directions; $P_c(\cos\theta)$ is the Legendre polynomial, and θ is the angle between $\boldsymbol{k}_a$ and $\boldsymbol{k}_e$ ($k_a=k_e$). The partial cross sections are

$$\sigma_c(k_i,k_f)=\pi\sum_{p=0}^{2j_i}(2p+1)\sum_{(J)=0}^{\infty}C(J_a'J_ac;1-10)C(J_e'J_ec;1-10)\begin{Bmatrix}J_a & J_a' & c\\ J_e' & J_e & p\end{Bmatrix}\times[J_a,J_a',J_e,J_e']\sum_{(\lambda)=0}^{1}(-1)^{p+c}(1+(-1)^{J_a+J_a'+\lambda_a+\lambda_a'+c})\beta_{pJ_aJ_e}^{\lambda_a\lambda_e}\beta_{pJ_a'J_e'}^{\lambda_a'\lambda_e'}{}^*,\quad(34)$$

where $[a,b,\ldots]=\sqrt{(2a+1)(2b+1)\cdots}$; we also used the notations

$$\beta_{0J_aJ_e}^{\lambda_a\lambda_e}=\delta_{J_e,J_a}\delta_{\lambda_a,\lambda_e}[N_e\alpha_{0J_aJ_a}^{\lambda_a\lambda_a}(n_i,\kappa_i)+(2j_c+1)\alpha_{0J_aJ_a}^{\lambda_a\lambda_a}(n_c,\kappa_c)], \tag{35}$$

$$\beta_{pJ_aJ_e}^{\lambda_a\lambda_e}=\sqrt{\frac{N_e(2j_i+1-N_e)}{2j_i}}\alpha_{pJ_aJ_e}^{\lambda_a\lambda_e}(n_i,\kappa_i),\quad p>0. \tag{36}$$

The radial parameters with $p=0$ are related to the parameters $M_{J,\lambda}$ of Eq. (23):

$$\alpha_{0JJ}^{\lambda\lambda}(n,\kappa)=\frac{4\pi}{2j+1}(-1)^{J+\lambda}\sqrt{2J+1}M_{J,\lambda}.$$

In fact there is only one surviving infinite summations in Eq. (34), due to the properties of 6-j symbols and Clebsch-Gordon coefficients. Parity conservation requires that $J_a+J_a'+J_e+J_e'+\lambda_a+\lambda_a'+\lambda_e+\lambda_e'$ be an even number. If an atom has more than one closed shell, one should coherently add amplitudes, weighted by the number of electrons present in the shells, to the right-hand side of Eq. (35).

The terms with $p>0$ in Eq. (34) describe contributions beyond the averaged-amplitude approximation, including all incoherent elastic scattering. It is seen from Eqs. (35),(36) that: (i) if the subshell is filled or empty, so that $N_e=2j_i+1$ or 0, then all terms with $p>0$ vanish. (ii) The scalar scattering cross section grows as the square of the total number of electrons, whereas the tensor scattering is the same for the case of one electron or one vacancy in the partially filled subshell, and is greatest for the case of a half-filled subshell. (iii) The averaged-amplitude approach works better the greater the number of electrons in closed shells.

By coherence we here have generally meant coherence between the different constituents of the atom. In Refs. [29,33,34] coherence between atoms, confined in a suitably small space relative to the wavelength of the scattered radiation, is also discussed. This is not a practical situation for the x-ray and γ-ray energies being considered here. However we note that such a situation would imply that the scalar part of the elastic scattering cross section (the averaged-amplitude result) would enter with a factor N^2, where N is the number of atoms from which scattering is taking place coherently, and so would be dominant, as in Refs. [29,33,34].

D. Further considerations of energy resolution

We finally mention that, if necessary, in addition to Raman scattering as in Eq. (20) one also can calculate inelastic Compton scattering. A general overview of the theories used in describing Compton scattering has recently been given [7]. Since this process is entirely incoherent (as is Raman scattering), there is no coherent summation over single-electron amplitudes, just as in the case of incoherent elastic scattering. The S-matrix approach has been applied to Compton scattering [6], and results using the impulse, incoherent-scattering factor, and A^2 approximations are also available (details are given in [7]). Though we concentrate in the following sections on coherent and incoherent elastic cross sections and on inelastic Raman cross sections for transitions between nearly-energy-degenerate states, a given finite energy resolution may imply other cross sections that are indistinguishable from the elastic cross section.

As an example of the role of experimental energy resolution in defining the processes included in an observed cross section, we refer to a recent experiment involving the scattering of 11-22 keV photons from neon [28]. (Since neon has only fully filled subshells the averaged-amplitude approach is appropriate for the elastic cross section.) In this case the cross sections were separated into elastic (Rayleigh) and inelastic (Compton) components. However, the energy resolution was such that the inelastic Raman cross section for transitions out of the L shell appeared with the elastic scattering, while the inelastic Raman cross section for transitions out of the more deeply bound K shell appeared with the inelastic Compton scattering. At lower energies even the inelastic Compton scattering is becoming indistinguishable from the elastic Rayleigh scattering.

III. ELASTIC SCATTERING FROM 2p EXCITED HYDROGEN

As an example of a case for which the effects of employing the averaged-amplitude approximation, instead of averaging cross sections over initial orientations and summing over final orientations, are substantial we consider elastic scattering from randomly oriented excited hydrogen atoms in the $2p$ state, with the final orientation of the target not being observed. Elastic photon scattering from the (nonrelativistically energy degenerate) $n=2$ states of atomic hydrogen has been analyzed using the nonrelativistic dipole approximation [14]. The target under consideration is a randomly oriented ensemble of excited atomic hydrogen atoms in the $2p$ state, with equal weight being given to each magnetic substate.

In the relativistic description the $2p$ subshell splits into the $2p_{1/2}$ and $2p_{3/2}$ subshells, whose relative populations in the ensemble will be according to their number of substates, since they are energetically very close together. The incident photon beam is unpolarized and we do not observe final photon polarizations or final target orientations. We shall not consider scattering for which the target ends up in the $2s$ state (the cross section for this is small, vanishing in the dipole approximation). We note that while in the nonrelativistic theory all the $n=2$ levels are energy degenerate, in the relativistic Dirac theory the $2s_{1/2}$ and $2p_{1/2}$ levels are energy degenerate, while the $2p_{3/2}$ level is less-deeply bound by $(\mathrm{Ryd}\,\alpha^2/16)=4.5\times10^{-5}$ eV, where Ryd is the Rydberg en-

ergy unit and α is the fine-structure constant (see, e.g., Ref. [35]). (The inclusion of radiative corrections in turn removes the degeneracy between the $2s_{1/2}$ and $2p_{1/2}$ levels.)

In providing a prediction to compare with an experimental result for scattering it is necessary to consider the implications of experimental details such as energy resolution. An experimental result purporting to correspond to the elastic scattering cross section in this situation may not have sufficient resolution in energy to resolve the splitting between the $2p_{1/2}$ and $2p_{3/2}$ levels, and it therefore would not distinguish between elastically scattered photons and inelastically scattered photons which correspond to a transition between these subshells. In this case one should compare with the sum of these elastic and inelastic cross sections. Indeed in the nonrelativistic theory these levels are energy degenerate, and so the ''elastic'' result within the nonrelativistic framework would correspond to this sum also.

Since the target is initially randomly oriented and final orientations are not being observed, coherent and incoherent elastic scattering cannot be distinguished, since one cannot say whether the atom has the exact same initial and final state or not. As discussed in the previous section, the averaged-amplitude approach gives the scalar coherent cross section for scattering, and is therefore only an approximation to the observable cross section (except for the case of closed-shell atoms where there is only scalar coherent elastic scattering).

Therefore the cross sections we are considering are (1) nonrelativistically, the nonrelativistic elastic cross section (coherent and incoherent) for transitions within the $2p$ subshell and (2) relativistically, the (properly weighted) elastic cross section (coherent and incoherent) for transitions within the $2p_{1/2}$ and $2p_{3/2}$ subshells, and the (incoherent) inelastic cross sections for Raman scattering involving transitions between these two subshells. These will be compared with the averaged-amplitude results.

In Ref. [14] numerical results are given for three atomic parameters *B*, *C*, and *D*, functions of energy only, that describe elastic photon scattering from excited hydrogen in the $2p$ state in the nonrelativistic dipole approximation. (A fourth parameter *A* describes elastic photon scattering from the $2s$ state; note that in the dipole approximation there is no two-photon $2p \leftrightarrow 2s$ transition.) The elastic scattering cross section (coherent and incoherent) in the nonrelativistic dipole approximation is given in terms of these parameters as

$$\frac{d\sigma}{d\Omega_{\text{elastic}}} = \frac{1}{2}[4B + (1+\cos^2\theta)(C+D)]r_0^2. \qquad (37)$$

The result obtained using the averaged-amplitude approach is

$$\frac{d\sigma}{d\Omega_{\text{ave amp}}} = \frac{1}{2}\left[(1+\cos^2\theta)\left(C + \frac{1}{3}(B+D)\right)\right]r_0^2. \qquad (38)$$

It corresponds to the (exact) result for elastic scattering in the case of a fully filled $2p$ subshell, though weighted according to the number of electrons actually present (one electron in our case). This corresponds to the scalar coherent cross section and is therefore an approximation to the elastic scattering cross section given in Eq. (37).

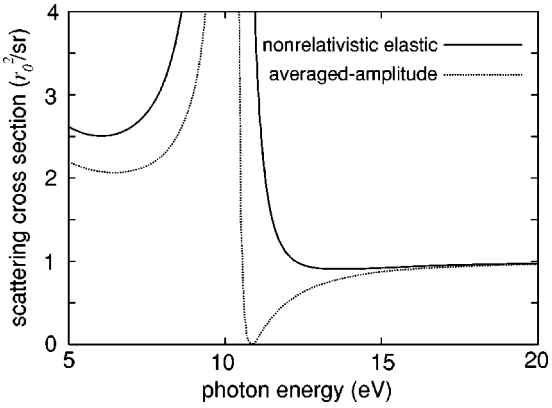

FIG. 1. Nonrelativistic cross sections for scattering at forward angle from $2p$ excited hydrogen. The elastic (coherent and incoherent) scattering cross section in the nonrelativistic theory is shown, together with averaged-amplitude result in the nonrelativistic theory.

In Fig. 1 the elastic cross section (coherent and incoherent) in the nonrelativistic dipole approximation for forward-angle scattering from excited hydrogen in the $2p$ state is shown, together with the averaged-amplitude result. Note that ''elastic'' here means elastic within the framework of the nonrelativistic theory, in which the $2p_{1/2}$ and $2p_{3/2}$ subshells are energy degenerate.

Turning now to the relativistic viewpoint, we show in Fig. 2 (for the same target, implying a weighting over the $2p_{1/2}$ and $2p_{3/2}$ subshells) the relativistic elastic cross section (coherent and incoherent) and the weighted (relativistically inelastic) Raman scattering cross sections corresponding to the atom making $2p_{1/2} \rightarrow 2p_{3/2}$ and $2p_{3/2} \rightarrow 2p_{1/2}$ transitions, which, though distinct cross sections, cannot be distin-

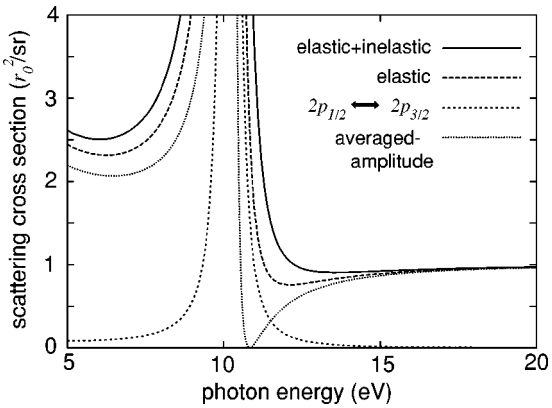

FIG. 2. Relativistic elastic (coherent and incoherent) cross section, and inelastic Raman cross sections for $2p_{1/2} \rightarrow 2p_{3/2}$ transitions and visa versa, together with their sum, for scattering at forward angle from $2p$ excited hydrogen. The weighted $2p_{1/2} \rightarrow 2p_{3/2}$ and $2p_{3/2} \rightarrow 2p_{1/2}$ inelastic Raman cross sections cannot be distinguished on the scale used. The averaged-amplitude result is also shown. The sum agrees with the nonrelativistic elastic cross section of Fig. 1; the averaged-amplitude results of the two figures also agree.

guished on the scale shown. The total cross section, appropriate for comparison with the nonrelativistic total elastic scattering cross section, is the sum of all these relativistic cross sections. (Note that there are details to consider in summing elastic and inelastic cross sections in this way to obtain a result corresponding to an ''elastic'' result in some limit—one should average over an appropriate energy resolution. How this is done can be important very close to resonances, where the cross sections are changing rapidly, but away from resonances one can simply add all the cross sections for the same initial photon energy, since they are changing slowly enough.)

Since we are in a regime where the nonrelativistic dipole approximation is valid we expect agreement between the nonrelativistic and relativistic approaches, if we are comparing appropriate cross sections, or sums of cross sections. The total cross section in Fig. 2 agrees with the nonrelativistic elastic cross section (shown in Fig. 1), and the averaged-amplitude results agree in the nonrelativistic and relativistic descriptions, confirming this. We see that the averaged-amplitude result can represent a poor approximation to the more correct results.

In obtaining the total cross section from the relativistic viewpoint it is therefore necessary to calculate the elastic cross section (coherent and incoherent) for the $2p_{1/2}$ and $2p_{3/2}$ subshells (properly averaged and weighted), and the Raman scattering cross sections in which the electron makes a transition from the $2p_{1/2}$ to the $2p_{3/2}$ subshell and visa versa. Therefore the nonrelativistic ''elastic'' cross section splits into the relativistic elastic cross section and the inelastic Raman scattering cross sections.

We now consider some of the characteristic features of the averaged-amplitude approach. As mentioned previously, this approach is exact only for fully filled subshells, being approximate for partially filled subshells. In our case of one electron in the $2p$ subshell it is seen to be a poor approximation. (Note that the averaged-amplitude approach does work well for ground-state hydrogen, even though the K shell is only half filled, since the corrections in this case are solely due to relativistic spin-flip effects, which are known to be small, though they become significant for high Z [21].) We see near zeroes above threshold in the averaged-amplitude cross section that are generally spurious for the case of partially filled subshells, (but real for configurations involving fully filled subshells, for which the averaged-amplitude description is appropriate). These near zeroes in the averaged-amplitude cross sections are associated with cancellations in the real part of the scattering amplitude when the single-particle amplitudes from all substates are summed—such cancellations do not occur in many configurations with partially filled subshells in the more correct approach in which the coherent cross sections are averaged for all definite magnetic substate occupations. For any given magnetic substate occupation one should coherently add only the single-particle amplitudes for the electrons present, which is only equivalent to coherently adding the amplitudes for all substates in the subshell when that subshell is fully filled. (Note these near zeroes are not true zeroes in the cross section due to the small but finite imaginary amplitude.)

Though the differences seem large for this case, it should be remembered that for many-electron atoms there are usually many electrons in fully filled subshells whose amplitudes must be added together to get the full elastic coherent amplitude, so that the effects of partially filled shells will generally be less important as percentage effects in the total cross section. This is considered in the next section.

IV. ELASTIC SCATTERING FROM MANY-ELECTRON ATOMS

As we saw in the previous section, the averaged-amplitude approach can be a poor approximation to the elastic (coherent and incoherent) scattering cross section for partially filled shells in the extreme case of a suitable (excited) one-electron atom. It should be remembered, though, that the averaged-amplitude S-matrix Rayleigh results have generally been used to describe elastic photon scattering for medium- to high-Z ground-state atoms for photon energies in the x-ray and γ-ray regime. In these situations there are many electrons present in fully filled subshells, which give rise to a large elastic coherent amplitude (for which the averaged amplitude is appropriate), and only the valence electrons in partially filled outer subshells are being treated approximately. Further, scattering from these valence electrons, again for photon energies in the x-ray and γ-ray regime, can usually be described using the (modified) form-factor approximation, for which there is no difference between the averaged-amplitude approach result and the more proper averaged cross section result at forward angle (and the incoherent elastic contribution vanishes at forward angle). With increasing angle the valence electron contribution drops rapidly compared to the (fully filled) inner shell contribution. Therefore we expect the averaged-amplitude approach to work well for these cases.

This suggests that for scattering from ground-state atoms, with photon energies exceeding the outer-electron thresholds, differences between the two approaches should be important only for low-Z atoms, where a greater fraction of the electrons are in partially filled subshells. For scattering from ground-state hydrogen the effects are not large because the effects in that case, associated with a half-filled K shell, are pure relativistic spin flip effects, known to be small for low Z [21] (the same is true for lithium, with a half-filled L_1 subshell). Therefore boron ($Z=5$) is the lowest-Z ground-state atom for which these effects can be significant.

In Fig. 3 we give results for scattering at forward angle from ground-state boron ($Z=5$), showing the relativistic elastic (coherent and incoherent) cross section. (Since the amplitudes are largely dipole dominant at all but the highest energies, we expect the features seen in and below the resonance region to persist at all angles.) Also shown are the inelastic incoherent Raman cross sections (properly weighted) for transitions between the L_2 and L_3 subshells and visa versa (which are distinct cross sections, but cannot be separately distinguished on the scale used). The sum of the elastic and inelastic cross sections is the total cross section, which corresponds to the total (coherent and incoherent) cross section obtained in a measurement or calculation

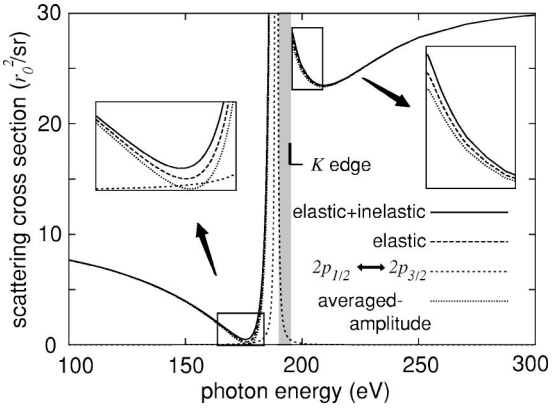

FIG. 3. Elastic (coherent and incoherent) cross section, and inelastic Raman cross sections for $2p_{1/2} \rightarrow 2p_{3/2}$ transitions and visa versa, together with their sum, for scattering at forward angle from ground-state boron. The weighted $2p_{1/2} \rightarrow 2p_{3/2}$ and $2p_{3/2} \rightarrow 2p_{1/2}$ inelastic Raman cross sections cannot be distinguished on the scale used. The averaged-amplitude result is also shown. The position of the *K* edge is indicated and details in the resonance region just below the *K* edge (shaded region) are omitted.

where the splitting between the L_2 and L_3 levels is not accounted for or resolved. The result for elastic scattering in the averaged-amplitude approach is also shown. The position of the *K* edge is indicated. The shaded area, just below the *K* edge, is a region of resonances from the *K* shell into all the unoccupied higher shells, forming a Rydberg sequence of resonances with the *K* edge as the accumulation point. The details of the resonant elastic cross section are omitted in this region.

Note that in some ways this situation is similar to the excited hydrogen case considered earlier, in that we have one electron in the $2p$ subshell. But we now have the coherent contribution of four other electrons in fully filled subshells, which drastically alters the overall picture. Whereas in the averaged-amplitude approach in the one-electron case there was a near zero in the cross section above the $1s \leftrightarrow 2p$ resonance, this is now only a shallow dip in the cross section, due to the contribution of the large coherent background amplitude (due to the four electrons in fully filled subshells). As the threshold is approached from above the real amplitudes are getting smaller in magnitude but approaching a finite value. Just above threshold the imaginary *K*-shell amplitude is large, causing the rise in the cross section as the threshold is reached. Thus, even for atoms with fully filled subshells, for which the averaged amplitude is correct, one can anticipate that there will be no near zeroes in the forward cross sections above threshold in neutral atoms—we have verified this for neon. For hollow atoms with electrons in fully filled subshells, as for example C $(2p^6)$, there can be real near zeroes above the downward $L \rightarrow K$ resonance transition.

However, below the $1s \leftrightarrow 2p$ resonance we now get a cancellation in the real amplitude between the rising resonant contribution in the *K*-shell amplitude associated with the $1s \rightarrow 2p$ resonance and the contribution of the *L*-shell electrons, giving rise to a near zero in the cross section. Note that these effects are seen in all cross sections in Fig. 3, already being present in the averaged-amplitude approach. At larger scattering angles we expect the near zero to occur at lower energy, to the extent that negative form-factor amplitudes involved in the cancellation are falling-off with increasing angle. Note that for high-*Z* atoms the situation is more complex as there will be many different subshell amplitudes involved with different fall-offs, but the resonance transition strengths involved (associated with the valence electrons) will be weaker.

Thus we see that, in boron, in the region well above its outer-shell threshold, going beyond the averaged-amplitude approach leads to comparatively small modifications to the cross section, partially washing out the near-zero below resonance, though the effect is only apparent at the bottom of the dip. Above the *K*-shell threshold one can also discern a difference between the results in the two approaches, but here the effects are relatively small compared with the overall magnitudes of the cross sections. The differences in the case of scattering from ground-state boron are of the same order as in excited hydrogen ($\lesssim 1 r_0^2$, both cases involving one electron in the $2p$ subshell). The effects in scattering from many-electron atoms as percentage effects on the averaged-amplitude cross section are generally small, due to the large coherent contribution involved, which is growing roughly with the square of the number of electrons present, but they can be important in the determination of anomalous scattering factors to high accuracy. However at the bottom of near-zero dips below thresholds the cross section can be many times the averaged-amplitude value. The proper understanding of these near zeroes is important, as they can be used to characterize scattering matrix elements [36], and they represent windows of transparency in scattering.

For scattering from ions and excited atoms there is always the possibility of having many of the electrons present in partially filled subshells, for any *Z*. In such cases the averaged-amplitude approach may be less successful in yielding accurate elastic scattering cross sections. The effect of interference between the scattering amplitudes from different partially filled subshells complicates the situation considerably, in particular in determining the locations, if any, of near zeroes in the cross sections. In particular one would expect additional effects in the case that there is a vacancy in one of the inner shells, or in the case of hollow atoms (with the inner shells completely vacant).

V. CONCLUSIONS

Circumstances have been identified in which simplified magnetic substate averaging at a matrix element level is inadequate. The approximation used in the usual *S* matrix formulation of elastic scattering, performing an average over magnetic substates at the level of the elastic coherent scattering amplitude, is justified for elastic scattering from randomly oriented many-electron ground-state atoms at energies above the inner electron thresholds, due to the dominant coherent contribution of the electrons in fully filled subshells. However, results for scattering from boron show that near zeroes below threshold in the averaged-amplitude cross section are partially filled-in in the more correct treatment, which includes incoherent elastic scattering and averaging

over orientations of the target at the level of the cross sections. Though these effects are otherwise generally small compared to the typical magnitudes of elastic scattering cross sections in many-electron atoms, they will still be important in the precision determination of anomalous scattering factors.

The averaged-amplitude approach is expected to be insufficient in cases where there is a large fraction of electrons in partially filled subshells, as in the extreme example of $2p$ excited hydrogen. In this case one also has to include inelastic scattering cross sections, involving transitions between the nearly energy degenerate $2p_{1/2}$ and $2p_{3/2}$ subshells, to obtain agreement with the results for elastic scattering obtained in the nonrelativistic theory. Lesser energy resolution would require including inelastic Raman cross sections for transitions into higher subshells, perhaps even the inelastic Compton cross section.

ACKNOWLEDGMENTS

This work was supported in part by the National Science Foundation under Grant Nos. PHY-9601752 and PHY-9970293, by the Russian Foundation for Basic Research under Grant No. 98-02-16111, and by INTAS-RFBR Grant No. IR 97-673.

APPENDIX A: MULTIPOLE EXPANSION

The multipole expansion of the photon operator $A=\boldsymbol{\alpha}\cdot\boldsymbol{\epsilon}e^{i\mathbf{k}\cdot r}$ is

$$A=\sum_{JM\lambda} C^{\lambda}_{JM}(\hat{\mathbf{k}},\boldsymbol{\epsilon})A^{\lambda}_{JM}(k,\mathbf{r}), \tag{A1}$$

where

$$C^{\lambda}_{JM}(\hat{\mathbf{k}},\boldsymbol{\epsilon})=4\pi i^{J-\lambda}(\mathbf{Y}^{(\lambda)}_{JM}(\hat{\mathbf{k}})\cdot\boldsymbol{\epsilon}),$$

$$A^{\lambda}_{JM}(k,\mathbf{r})=\boldsymbol{\alpha}\cdot\mathbf{a}^{\lambda}_{JM}(k,\mathbf{r}), \tag{A2}$$

and

$$\mathbf{a}^{\lambda=0}_{JM}(k,\mathbf{r})=j_J(kr)\mathbf{Y}_{JJM}(\hat{\mathbf{r}}), \tag{A3}$$

$$\mathbf{a}^{\lambda=1}_{JM}(k,\mathbf{r})=\sqrt{\frac{J+1}{2J+1}}j_{J-1}(kr)\mathbf{Y}_{JJ-1M}(\hat{\mathbf{r}}) - \sqrt{\frac{J}{2J+1}}j_{J+1}(kr)\mathbf{Y}_{JJ+1M}(\hat{\mathbf{r}}).$$

In scattering there is an absorbed and emitted photon, and the quantity $C^{\lambda_a}_{J_aM_a}(\hat{\mathbf{k}}_a,\boldsymbol{\epsilon}_a)C^{\lambda_e *}_{J_eM_e}(\hat{\mathbf{k}}_e,\boldsymbol{\epsilon}_e)$ is needed. Note that in general it is not trivial to give explicit expressions for this quantity, and here we consider certain special cases. The photon polarization vectors are written in the form $\boldsymbol{\epsilon}=\epsilon^{+}\hat{\boldsymbol{\epsilon}}^{+}+\epsilon^{-}\hat{\boldsymbol{\epsilon}}^{-}$, where $\hat{\boldsymbol{\epsilon}}^{+}$ ($\hat{\boldsymbol{\epsilon}}^{-}$) corresponds to right-handed (left-handed) circular polarization.

In the case of the averaged-amplitude approach only the diagonal terms in the product of the multipole expansions of the two photon operators survive, for which $(J_aM_a\lambda_a=J_eM_e\lambda_e=JM\lambda)$

$$\sum_M C^{\lambda=1}_{JM}(\hat{\mathbf{k}}_a,\boldsymbol{\epsilon}_a)C^{\lambda=1*}_{JM}(\hat{\mathbf{k}}_e,\boldsymbol{\epsilon}_e) = \frac{2J+1}{8\pi}[(\epsilon_i^{+}\epsilon_f^{+*}+\epsilon_i^{-}\epsilon_f^{-*})U_J + (\epsilon_i^{+}\epsilon_f^{-*}+\epsilon_i^{-}\epsilon_f^{+*})V_J], \tag{A4}$$

$$\sum_M C^{\lambda=0}_{JM}(\hat{\mathbf{k}}_a,\boldsymbol{\epsilon}_a)C^{\lambda=0*}_{JM}(\hat{\mathbf{k}}_e,\boldsymbol{\epsilon}_e) = \frac{2J+1}{8\pi}[(\epsilon_i^{+}\epsilon_f^{+*}+\epsilon_i^{-}\epsilon_f^{-*})V_J + (\epsilon_i^{+}\epsilon_f^{-*}+\epsilon_i^{-}\epsilon_f^{+*})U_J],$$

where

$$U_J=\pi_J+\tau_J, \quad V_J=\pi_J-\tau_J, \tag{A5}$$

and

$$\pi_J=\frac{1}{J(J+1)}\frac{dP_J(\cos\theta)}{d\cos\theta}=\frac{1}{2}\left[\frac{P_{J-1}(\cos\theta)+P_{J+1}(\cos\theta)}{2} + \frac{P^2_{J-1}(\cos\theta)+P^2_{J+1}(\cos\theta)}{2J(J+1)}\right],$$

$$\tau_J=\frac{1}{J(J+1)}\frac{dP^1_J(\cos\theta)}{d\theta}=\frac{1}{2}\left[P_J(\cos\theta)-\frac{P^2_J(\cos\theta)}{J(J+1)}\right]. \tag{A6}$$

We also give explicit results for the case of the electric dipole amplitude $(J_a=J_e=1,\lambda_a=\lambda_e=1)$:

$$C^{1}_{1M_a=\pm1}(\hat{\mathbf{k}}_a,\boldsymbol{\epsilon}_a)C^{1*}_{1M_e=1}(\hat{\mathbf{k}}_e,\boldsymbol{\epsilon}_e) = \left(\frac{3}{8\pi}\right)\left[\epsilon_i^{\pm}\epsilon_f^{+*}\frac{1}{2}(1+\cos\theta)+\epsilon_i^{\pm}\epsilon_f^{-*}\frac{1}{2}(1-\cos\theta)\right],$$

$$C^{1}_{1M_a=\pm1}(\hat{\mathbf{k}}_a,\boldsymbol{\epsilon}_a)C^{1*}_{1M_e=0}(\hat{\mathbf{k}}_e,\boldsymbol{\epsilon}_e) = \left(\frac{3}{8\pi}\right)[\epsilon_i^{\pm}\epsilon_f^{+*}-\epsilon_i^{\pm}\epsilon_f^{-*}]\sin\theta, \tag{A7}$$

$$C^{1}_{1M_a=\pm1}(\hat{\mathbf{k}}_a,\boldsymbol{\epsilon}_a)C^{1*}_{1M_e=-1}(\hat{\mathbf{k}}_e,\boldsymbol{\epsilon}_e) = \left(\frac{3}{8\pi}\right)\left[\epsilon_i^{\pm}\epsilon_f^{+*}\frac{1}{2}(1-\cos\theta)+\epsilon_i^{\pm}\epsilon_f^{-*}\frac{1}{2}(1+\cos\theta)\right],$$

with terms involving $M_a=0$ vanishing.

APPENDIX B: ANGULAR INTEGRALS

The following angular integral appears in the multipole decomposed scattering amplitude [5]:

$$I^{JM}_{\kappa' m', \kappa m} = \int d\Omega\, \Omega^{\dagger}_{\kappa' m'} Y_{JM} \Omega_{\kappa m}$$
$$= (-1)^{(J+j-j')} \sqrt{\frac{(2J+1)(2j+1)}{4\pi(2j'+1)}}$$
$$\times C\left(jJj'; \frac{1}{2}0\frac{1}{2}\right) C(jJj'; mMm') \Pi_{lJl'}, \tag{B1}$$

where $\Pi_{lJl'}=1$ if $(l+J+l')$ is even and is zero otherwise. We note the following properties:

$$I^{JM}_{\kappa' m', \kappa m} = I^{JM}_{-\kappa' m', -\kappa m}, \quad I^{JM}_{\kappa' m', \kappa m} = (-1)^M I^{J-M}_{\kappa m, \kappa' m'}, \tag{B2}$$

and the following result, used in deriving the scattering amplitude in the averaged-amplitude approximation:

$$\sum_{mm'} I^{JM}_{\kappa' m', \kappa m} I^{J' M'}_{\kappa' m', \kappa m} = \frac{(2j+1)}{4\pi} C^2\left(jJj'; \frac{1}{2}0\frac{1}{2}\right) \Pi_{lJl'} \delta_{JJ'} \delta_{MM'}. \tag{B3}$$

[1] R. H. Pratt, L. Kissel, and P. M. Bergstrom, Jr., in *X-ray Anomalous (Resonance) Scattering: Theory and Experiment*, edited by K. Fischer, G. Materlik, and C. Sparks (Elsevier, Amsterdam, 1994), pp. 9–33.

[2] P.P. Kane, L. Kissel, R.H. Pratt, and S.C. Roy, Phys. Rep. **140**, 75 (1986).

[3] L. Kissel, Ph.D. thesis, University of Pittsburgh, 1977.

[4] G.E. Brown, R.E. Peierls, and J.B. Woodward, Proc. R. Soc. London, Ser. A **227**, 51 (1955).

[5] W.R. Johnson and F.D. Feiock, Phys. Rev. **168**, 22 (1968).

[6] P.M. Bergstrom, Jr., T. Surić, K. Pisk, and R.H. Pratt, Phys. Rev. A **48**, 1134 (1993).

[7] P.M. Bergstrom, Jr. and R.H. Pratt, Radiat. Phys. Chem. **50**, 3 (1997).

[8] L. Kissel, B. Zhou, S.C. Roy, S.K. Sen Gupta, and R.H. Pratt, Acta Crystallogr., Sect. A: Found. Crystallogr. **51**, 271 (1995).

[9] S.C. Roy, B. Sarkar, L. Kissel, and R.H. Pratt, Phys. Rev. A **34**, 1178 (1986).

[10] A. Costescu, P.M. Bergstrom, Jr., C. Dinu, and R.H. Pratt, Phys. Rev. A **50**, 1390 (1994).

[11] P.M. Bergstrom, Jr., L. Kissel, R.H. Pratt, and A. Costescu, Acta Crystallogr., Sect. A: Found. Crystallogr. **53**, 7 (1997).

[12] M. Gavrila, Z. Phys. A **163**, 147 (1967).

[13] A. Costescu, Rev. Roum. Phys. **21**, 3 (1976).

[14] M. Gavrila, Z. Phys. A **293**, 269 (1979).

[15] A. Cionga and V. Florescu, Z. Phys. D **2**, 49 (1986).

[16] V. Florescu and A. Cionga, Z. Phys. A **321**, 187 (1985).

[17] B.A. Zon, N.L. Manakov, and L.P. Rapoport, Zh. Exp. Teor. Fiz. **55**, 924 (1968) [Sov. Phys. JETP **28**, 480 (1968)].

[18] M. Gavrila and A. Costescu, Phys. Lett. **28A**, 614 (1969).

[19] M. Gavrila and A. Costescu, Phys. Rev. A **2**, 1752 (1970).

[20] V. Florescu and M. Gavrila, Phys. Rev. A **14**, 211 (1976).

[21] V. Florescu, M. Marinescu, and R. H. Pratt, Phys. Rev. A **42**, 3844 (1990).

[22] N.L. Manakov, A.A. Nekipelov, and A.G. Fainshtein, Yad. Fiz. **45**, 1091 (1987) [Sov. J. Nucl. Phys. **45**, 677 (1987)].

[23] J.H. Hubbell, Wm.J. Veigele, E.A. Briggs, R.T. Brown, D.T. Cromer, and R.J. Howerton, J. Phys. Chem. Ref. Data **4**, 471 (1975).

[24] J.H. Hubbell and I. Øverbø, J. Phys. Chem. Ref. Data **8**, 69 (1979).

[25] D. Schaupp, M. Schumacher, F. Smend, and P. Rullhusen, J. Phys. Chem. Ref. Data **12**, 467 (1983).

[26] Various results for elastic photon-atom scattering based on form factors and form factors combined with anomalous scattering factors are available interactively online at http://www-phys.llnl.gov/V_Div/scattering/elastic.html. *S*-matrix results are also available on a fixed grid.

[27] B.K. Chatterjee and S.C. Roy, J. Phys. Chem. Ref. Data **27**, 1011 (1998).

[28] M. Jung, R.W. Dunford, D.S. Gemmell, E.P. Kanter, B. Krässig, T.W. LeBrun, S.H. Southworth, L. Young, J.P.J. Carney, L. LaJohn, R.H. Pratt, and P.M. Bergstrom, Jr., Phys. Rev. Lett. **81**, 1596 (1998).

[29] V.B. Berestetskii, E.M. Lifshitz, and L.P. Pitaevskii, *Quantum Electrodynamics* (Pergamon Press, Oxford, 1982).

[30] D. Gibbs, D.E. Moncton, K.L. D'Amico, J. Bohr, and B.H. Grier, Phys. Rev. Lett. **55**, 234 (1985).

[31] N.L. Manakov, A.V. Meremianin, A. Maquet, J.P.J. Carney, and R. H. Pratt (unpublished).

[32] N.L. Manakov, V.D. Ovsiannikov, and S. Kielich, Acta Phys. Pol. A **53**, 581 (1978).

[33] M.Ya. Agre and L.P. Rapoport, Zh. Éksp. Teor. Fiz. **104**, 2975 (1993) [Sov. Phys. JETP **77**, 382 (1993)].

[34] M.Ya. Agre and L.P. Rapoport, Zh. Éksp. Teor. Fiz. **109**, 1203 (1996) [Sov. Phys. JETP **82**, 647 (1996)]; [**83**, 414(E) (1996)].

[35] H.A. Bethe and E.E. Salpeter, *Quantum Mechanics of One- and Two-Electron Atoms* (Plenum, New York, 1977).

[36] M.D. Havey, Phys. Lett. A **240**, 219 (1998).